Am J Transl Res 2017;9(8):3723-3731
www.ajtr.org /ISSN:1943-8141/AJTR0054142

Original Article

Image-guided stem cells with functionalized self-assembling peptide nanofibers for treatment of acute myocardial infarction in a mouse model

Xiao Li[1*], Ying-Ying Chen[2*], Xiu-Mei Wang[2], Kai Gao[3], Yun-Zhou Gao[4], Jian Cao[1], Zhuo-Li Zhang[5], Jing Lei[1], Zheng-Yu Jin[1], Yi-Ning Wang[1]

[1]Department of Radiology, Peking Union Medical College Hospital, Chinese Academy of Medical Sciences and Peking Union Medical College, Beijing 100730, China; [2]Key Laboratory of Advanced Materials, School of Materials Science and Engineering, Tsinghua University, Beijing 100084, China; [3]Institute of Laboratory Animal Sciences, Chinese Academy of Medical Sciences and Peking Union Medical College, Beijing 100021, China; [4]Department of Pathology and Center for Experimental Animal Research, Institute of Basic Medical Sciences, Chinese Academy of Medical Sciences and Peking Union Medical College, Beijing 100005, China; [5]Department of Radiology, Feinberg School of Medicine, Northwestern University, Chicago, IL 60611, USA. [*]Equal contributors.

Received March 29, 2017; Accepted July 11, 2017; Epub August 15, 2017; Published August 30, 2017

Abstract: Aim: To investigate the survival of bone marrow mesenchymal stem cells (BMSCs) and the therapeutic effect for acute myocardial infarction (AMI) after co-transplantation with the functionalized self-assembling peptide nanofiber RAD/PRG or RAD/KLT. Methods: AMI of balb/c mice was induced. Mice were randomly divided into four groups, and received treatment of phosphate buffered saline (PBS) (Group A), GFP/Fluc-BMSCs (Group B), GFP/Fluc-BMSCs + RAD/PRG (Group C), and GFP/Fluc-BMSCs + RAD/KLT (Group D), respectively. Bioluminescence imaging (BLI) was performed on day 1 (d-1), d-4, d-7, d-10, and d-13 after transplantation. Magnetic resonance imaging (MRI) was performed at baseline (d-4 before transplantation) and d-29 after treatment. Mice were euthanized on d-29 following treatment. Paraffin sections were obtained from the top, mid and bottom part of the infarcted region along the long-axis of the heart. Hematoxylin and eosin (HE) staining and immunohistochemical staining were performed. The infarct ratio micro-vascular density (MVD) was quantified. Results: There was a significant higher of BLI signal intensity of BMSCs in Group C than that in Group B (d-4, 9713±320 vs. 8164±378, P=0.0008; d-7, 6489±241 vs. 5417±361, P=0.0026; d-10, 3768±255 vs. 0, P < 0.0001). The left ventricular ejection fraction (LVEF) via MRI examination was significantly improved in both Group C and Group D. Infarct ratio and MVD were significantly improved in both Group C and Group D. Conclusion: Our data highlights BMSCs combining functionalized self-assembling peptide nanofibers RAD/PRG or RAD/KLT as promising therapy for AMI.

Keywords: Stem cell therapy, functionalized self-assembling peptide nanofibers, molecular imaging, acute myocardial infarction

Introduction

Stem cell therapies have been explored to treat myocardial infarction (MI) and related heart failure by improving cardiac repair and ventricular remodeling. Preclinical and clinical trials of mesenchymal stem cells (MSCs) [1], cardiac stem cells (CSCs) [2], and skeletal myoblasts (SMs) [3] have produced promising results. Bone marrow-derived mesenchymal stem cells (BMSCs) are unique due to their pluripotent capacity, paracrine ability, lower immunogenicity and better maneuverability [4, 5]. Gaining insight into the underlying biological behavior and functional mechanism of transplanted stem cells *in vivo* remains a primary unresolved issue. Based on various probes and devices, molecular imaging enables non-invasive, longitudinal, semi-quantitative tracing of transplanted stem cells. There is no ideal method; thus, dual-modal or multi-modal molecular imaging has become increasingly accepted to obtain a full understanding and assessment of stem cell therapy with comprehensive information [6].

According to recent studies, the long-term survival of stem cells after transplantation is not idea land a consistent therapeutic effect remains controversial [7, 8]. Inflammation of ischemia/reperfusion (I/R) injury plays a critical role in the stem cell therapy as evidenced by the experimental and clinical studies [8, 9]. Therefore, efforts have been made to provide a better living environment for stem cells. RADA-16-I (Ac-$(RADA)_4$-$CONH_2$) is a type of injectable self-assembling peptide nanofiber shown to support the attachment, growth and differentiation of stem cells and mature somatic cells *in vitro* and *in vivo* [10]. Furthermore, RADA16-I can be functionalized by adding functional peptides to its C-terminal end. One type of functional peptide, PRG (Ac-$(RADA)_4$GPRGDSGYRGDS-$CONH_2$), contains RGD, which is a natural cell adhesion motif to regulate the localization and proliferation of cells by ligation with integrin. Another functional peptide, KLT (Ac-$(RADA)_4G_4$KLTWQELYQLKYKGI-$CONH_2$), enhances angiogenesis by mimicking vascular endothelial growth factor (VEGF) [11]. The bioactivities of PRG and KLT *in vitro* have been proven in vitro [11, 12], and their biocompatibilities *in vivo* have been recognized [13].

A feasible dual-modal imaging system *in vivo* using bioluminescence imaging (BLI) and magnetic resonance imaging (MRI) has been established to track the transplanted stem cells and evaluate their therapeutic efficiency [14]. In this study, we aim to promote the localization, survival, and therapeutic effect of stem cells by co-transplantation with the functionalized self-assembling peptide nanofiber RAD/PRG or RAD/KLT, an activity that has not yet been examined by dual-modal imaging of BLI and MRI *in vivo*.

Materials and methods

The Institutional Committee for Animal Welfare and Ethnics at Peking Union Medical College Hospital (Beijing, China) approved all animal experiments that were performed in accordance with the relevant guidelines and regulations.

GFP/Fluc BMSC culture

BMSCs stably expressing green fluorescence protein and firefly luciferase (GFP/Fluc) were purchased from Cyagen Biosciences (RAFMX-01201; Guangzhou, Guangdong Province, China). BMSCs were extracted from SD rats (p3, RASMC-01001; Guangzhou, Guangdong Province, China). Passage 5 GFP/Fluc-BMSCs at an undifferentiated state were used.

Peptide solution preparation

The self-assembling peptide RADA16-I (Ac-$(RADA)_4$-$CONH_2$), functionalized peptide PRG (Ac-$(RADA)_4$GPRGDSGYRGDS-$CONH_2$) and KLT (Ac-$(RADA)_4G_4$KLTWQELYQLKYKGI-$CONH_2$) were synthesized by China Peptides (Shanghai, China). The peptides were dissolved in sterilized water at a concentration of 1% (10 mg/ml, w/v). All of the peptide solutions were sonicated for 30 minutes and filtered by a 0.22 um syringe filter. PRG solution or KLT solution were separately mixed with RADA16-I solution at a volume ratio of 1:1 to obtain either a RAD/PRG solution or RAD/KLT solution. After injection into the myocardium, the peptide solutions convert to hydrogels at physiological pH and form a 3-D network of 10-nm fiber diameter, with 5 to 200-nm pore size and more than 99% water content. This structure physically mimics the natural extracellular matrix and provides a beneficial living environment for stem cells *in vivo* [15].

Acute myocardial infarction (AMI) model and GFP/Fluc BMSC transplantation

Balb/c mice (females, weighting 18-20 g; Beijing HFK Bioscience Co. Ltd., Beijing, China) were anesthetized by an intra-peritoneal injection of 10% chloral hydrate (0.03 mg/kg), and were then intubated and mechanically ventilated. After the thoracic cavity and pericardium were opened, the left anterior descending coronary artery was ligated permanently using a 7-0 silk suture. Mice were randomly divided into Groups A (control), B, C and D. Group A served as control group and received phosphate buffered saline (PBS); Group B was treated by GFP/Fluc-BMSCs; Group C was treated by GFP/Fluc-BMSCs + RAD/PRG; and Group D was treated by GFP/Fluc-BMSCs + RAD/KLT, respectively. For Group B, GFP/Fluc-BMSCs were suspended in PBS at a concentration of 1.0×10^6/ml; for Groups C and D, GFP/Fluc-BMSCs were suspended in RAD/PRG or RAD/KLT solution at the same concentration. Immediately after suspension, 40 ul was injected into two regions around the border of the infarcted myocardium through a 30-gauge insulin springe.

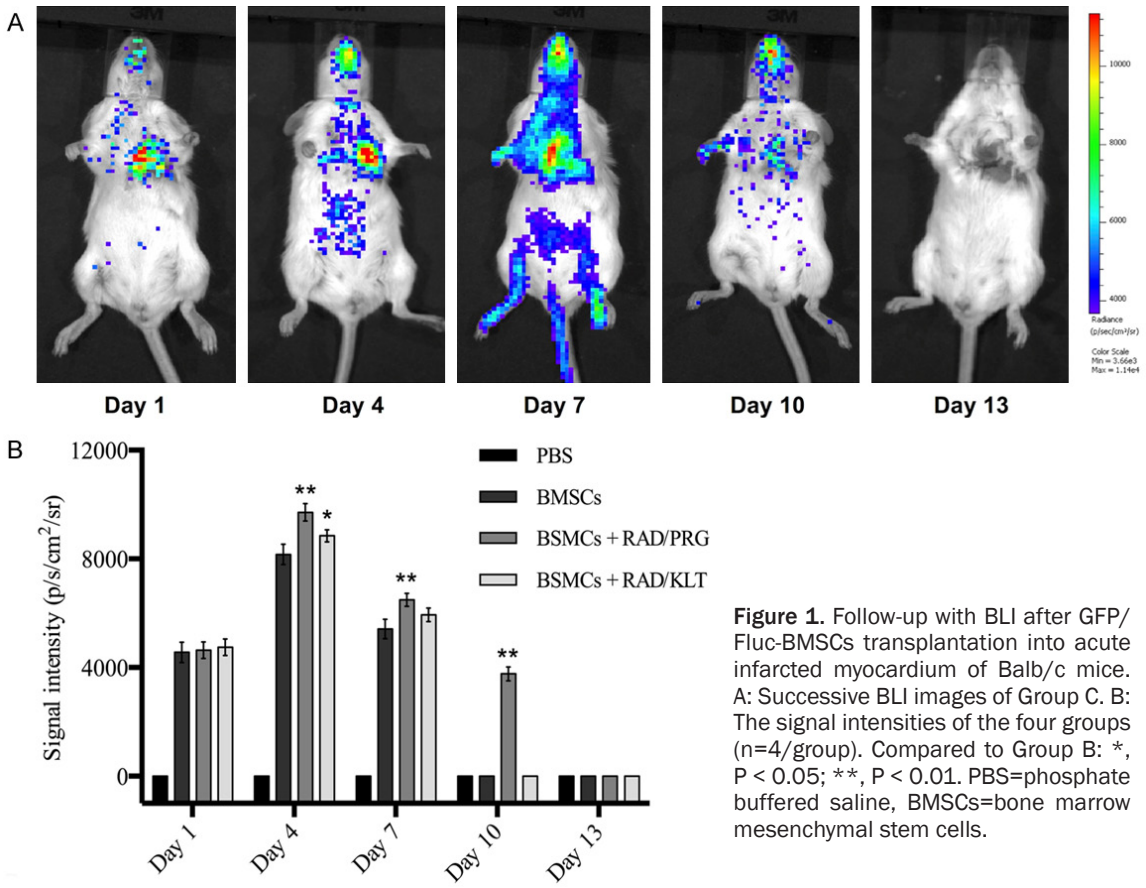

Figure 1. Follow-up with BLI after GFP/Fluc-BMSCs transplantation into acute infarcted myocardium of Balb/c mice. A: Successive BLI images of Group C. B: The signal intensities of the four groups (n=4/group). Compared to Group B: *, $P < 0.05$; **, $P < 0.01$. PBS=phosphate buffered saline, BMSCs=bone marrow mesenchymal stem cells.

BLI to trace GFP/Fluc-BMSCs in vivo

BLI was performed on days 1, 4, 7, 10, and 13 following transplantation until the detected optical signal of all groups fell below the threshold level at day 13. After anesthetization with 2% isoflurane, each mouse received an intraperitoneal injection of D-luciferin solution (luc-001, Sciencelight, Berthold Technologies, Bad Wildbad, Germany) at a concentration of 15 mg/ml and at a dose of 250 mg/kg body weight. Immediately after injection, a series of bioluminescent images was acquired at a 2-minute interval for approximately 20 minutes using the NightOWL LB 983 *in vivo* Imaging System (Berthold Technologies, Bad Wildbad, Germany). For the image of the peak signal intensity, an ROI was drawn on the heart region and expressed as p/s/cm^2/sr. Data were analyzed by two observers with 2 years of experience independently.

MRI to evaluate cardiac function

MRI was performed at baseline (4 days before transplantation), and on days 3 and 28 following transplantation. After anesthetization with 2% isoflurane, electrocardiography, respiration, and the core temperature of mice were monitored using an MRI-compatible system (SA Instruments, Stony Brook, NY, USA). Successive short-axis slices to cover the left ventricle from the apex to the base were acquired using a cardiac CINE sequence on a Varian 7.0T small animal magnetic resonance scanner (Varian, Palo Alto, CA, USA). The parameters were as follows: TR: 127.4 ms; TE: 2.85 ms; thickness: 1 mm; FOV: 10×10 mm; Matrix: 192×192; FA: 20°. For each mouse, the left ventricular ejection fraction (LVEF) was quantified using Argus software (Siemens Medical Solution, Erlangen, Germany) by two radiologists with 3 years of experience independently.

Histological examination

Mice were euthanized on day 29. Paraffin sections were obtained from the top, mid and bottom part of the infarcted region along the long-axis of the heart. Hematoxylin and eosin (HE) staining and immunohistochemical analyses of

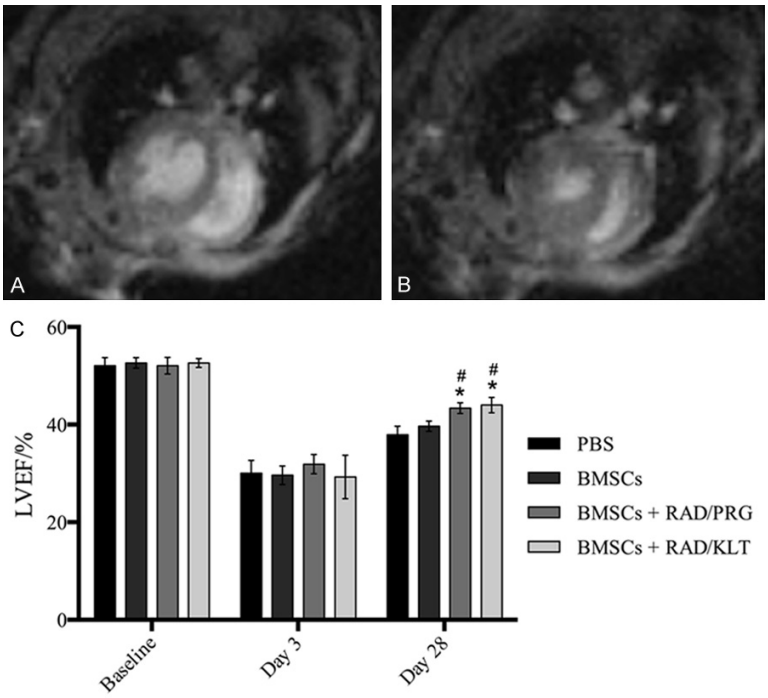

Figure 2. Follow-up with MRI after GFP/Fluc-BMSCs transplantation into acute infarcted myocardium of Balb/c mice. Short-axis cardiac MRI images of Group B on day 28 at end-diastolic stage (A) and end-systolic stage (B). (C) The LVEFs of the four groups (n=3/group). Compared to Group A: *, P < 0.05. Compared to Group B: #, P < 0.05. PBS=phosphate buffered saline, BMSCs=bone marrow mesenchymal stem cells, LVEF=left ventricular ejection fraction.

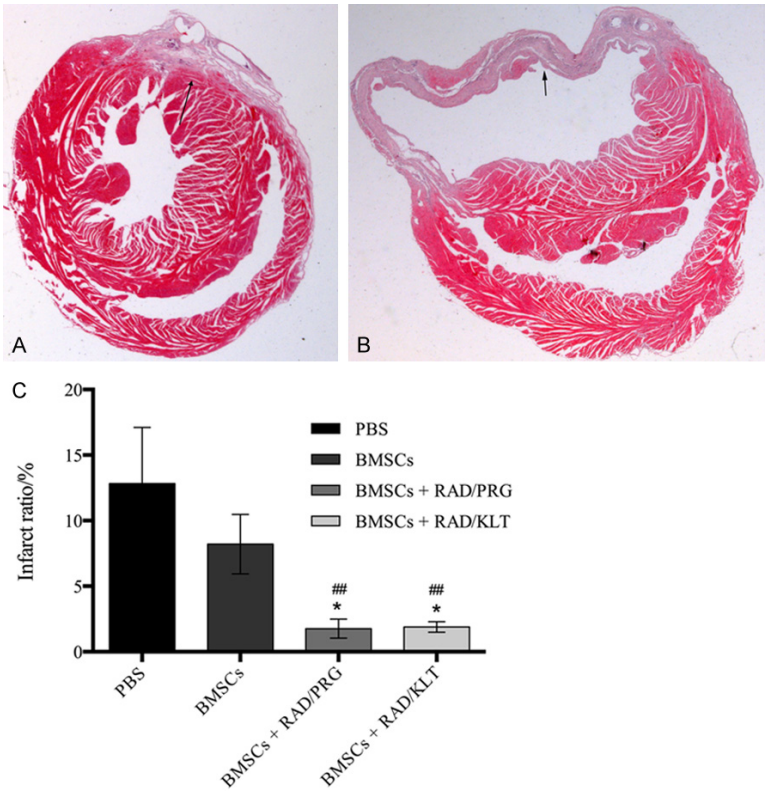

Figure 3. HE staining and infarct ratios of the acute infarcted myocardium of Balb/c mice. HE staining (10×) cross sections of Groups C (A) and (A B). The myocardium was replaced by fibrous scar tissue (black arrow) within the infarcted foci of left ventricle. (C) The infarct ratios of the four groups (n=3/group). Compared to Group A: *, P < 0.05. Compared to Group B: ##, P < 0.01. PBS=phosphate buffered saline, BMSCs=bone marrow mesenchymal stem cells.

GFP (rabbit anti-GFP antibody; 50430-2-AP; ProteinTech, Chicago, USA) and CD34 (rabbit anti-CD34 antibody, 14486-1-AP, ProteinTech, Chicago, USA) were performed. The infarct ratio (average of infarct size/total size of the left and right ventricles multiply the length) was quantified according to HE staining using Image-pro Plus software (Media Cybernetics, Bethesda, MD, USA). Micro-vascular density (MVD) was also quantified using Image-pro Plus software according to CD34 positive cells.

Statistical analysis

The SPSS 15.0 (IBM SPSS, NY, USA) statistical program was used. Data were presented as the mean ± standard deviation. Normal distribution was proven by the Shapiro-Wilk test, and data were compared by one-way analysis of variance (ANOVA). P < 0.05 was considered statistically significant.

Results

BLI to trace GFP/Fluc-BMSCs in vivo

A dynamic follow-up by BLI of Group C is shown in **Figure 1A** as an example, and the signal intensities of the four groups (n=4/group) are shown in

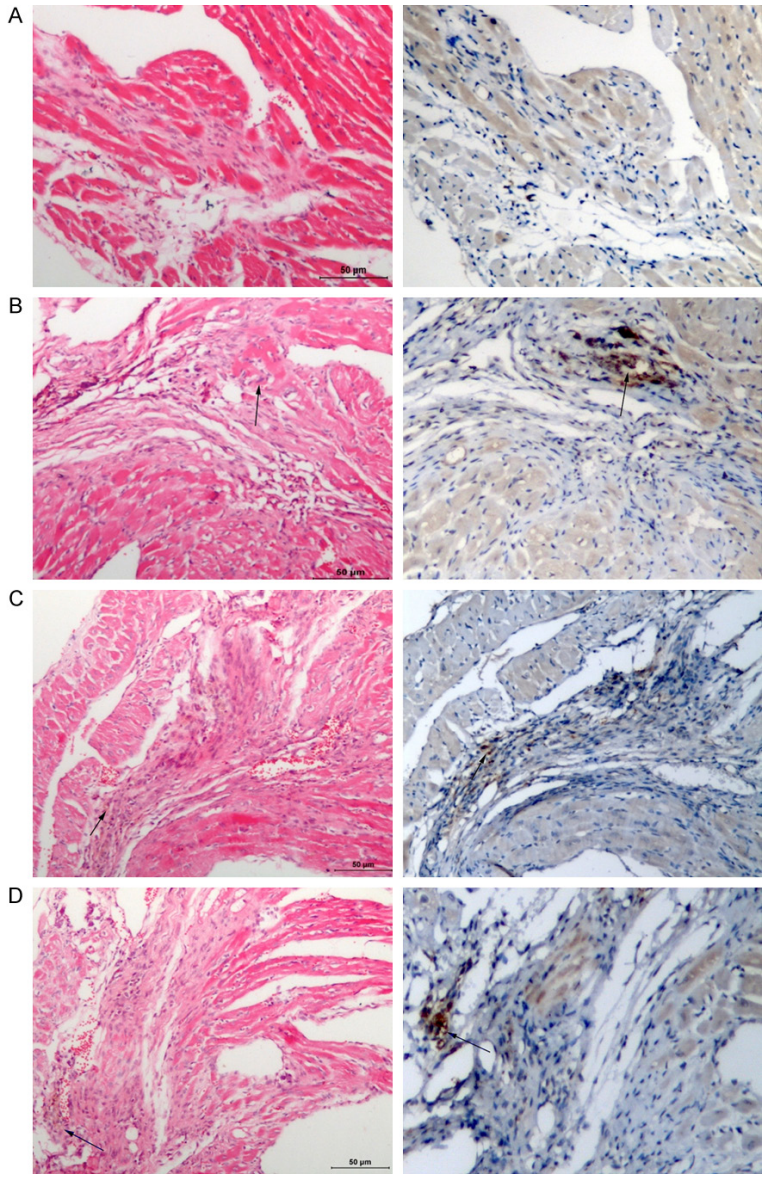

Figure 4. HE staining and GFP immunohistochemical analysis of the acute infarcted myocardium of Balb/c mice. A: HE staining and GFP immunohistochemical analysis of Group A (100×). B: HE staining and GFP immunohistochemical analysis of Group B (100×) showed GFP positive clustering cardiomyocytes (black arrow). C: HE staining and GFP immunohistochemical analysis of Group C (100×) showed rich mature vessels and GFP positive cells (black arrow). D: HE staining and GFP immunohistochemical analysis of Group D (100×) showed rich mature vessels and GFP positive cells (black arrow).

Figure 1B. BLI signals were detected in the cardiac region of Groups B, C and D on day 1 after transplantation, and peaked on day 4; but decreased since day 7. The signals of Groups B and D fell below the detection threshold on day 10, and that of Group C fell below the detection threshold on day 13, indicating that few bioactive GFP/Fluc-BMSCs remained in the heart. No signal could be detected from Group A. The signal intensity of Group C was significantly higher than that of Group B since day 4 (day 4, 9713±320 vs. 8164±378, P=0.0008; day 7, 6489±241 vs. 5417±361, P=0.0026; day 10, 3768±255 vs. 0, P < 0.0001), indicating that co-transplantation with RAD/PRG promoted the localization and survival of GFP/Fluc-BMSCs *in vivo*. The signal intensity of Group D was higher than that of Group B only on day 4 (8851±223 vs. 8164±378, P=0.0202), indicating that co-transplantation with RAD/KLT provided no benefit. BLI signals were also detected in the cardiac region in Groups B, C and D, indicating the distribution of GFP/Fluc-BMSCs throughout the whole body.

MRI to evaluate cardiac function

Images of cardiac MRI from Group B on day 28 are shown in **Figure 2A** and **2B** as examples, and the LVEF values of the four groups (n=3/group) are shown in **Figure 2C**. At baseline, there was no significant difference in the LVEF values among the four groups (P=0.9133). On day 3 after transplantation, the LVEF values of the four groups were all reduced, with no significant difference among them (P=0.7048). On day 28, the LVEF values of the four groups were all improved; but still lower than baseline value. There was no significant difference between Groups A and B (P=0.2121), indicating that treatment with GFP/Fluc-BMSCs alone had no therapeutic effect. The LVEF values of Groups C and D were higher than those of Groups A (43.37±1.12% vs. 37.93±1.72%, P=0.0102; 44.00±1.57% vs. 37.93±1.72%, P=0.0108) and B (43.37±1.12% vs. 39.67±1.06%, P=0.0141; 44.00±1.57% vs. 39.67±1.06%,

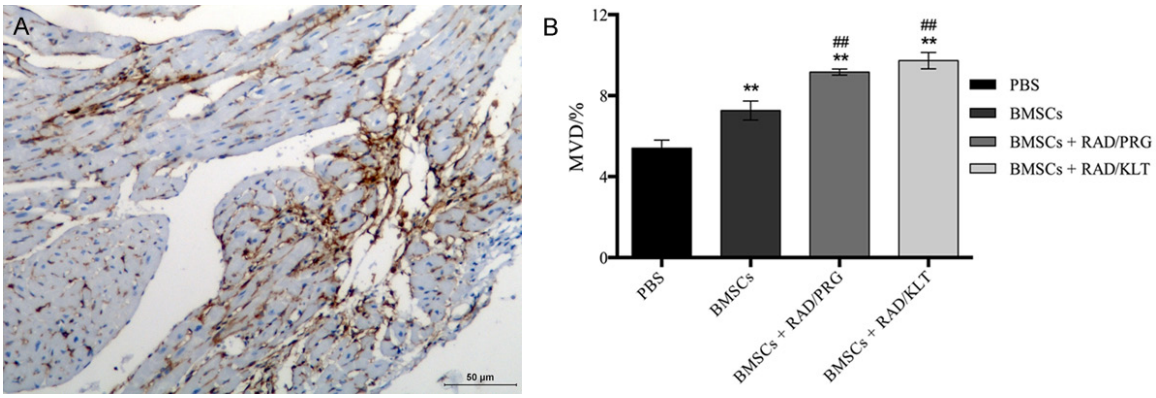

Figure 5. Immunohistochemical analysis of CD34 and the MVDs of the acute infarcted myocardium of Balb/c mice. A: Immunohistochemical analysis of CD34 (100×) from Group A showed increased CD34-positive cells within infarcted foci than normal myocardium. B: The MVDs of the four groups (n=3/group). Compared to Group A: **, P < 0.01. Compared to Group B: ##, P < 0.01. PBS=phosphate buffered saline, BMSCs=bone marrow mesenchymal stem cells, MVD=micro-vascular density.

P=0.0167), indicating that co-transplantation with RAD/PRG or RAD/KLT could both improve the outcome. There was no significant difference between Group C and D (P=0.5996).

Histological examination

HE staining (10×) of cross sections from Groups C and A are shown in **Figure 3A** and **3B** as examples, and the infarct ratios of the four groups are displayed in **Figure 3C**. The myocardium was replaced by fibrous scar tissue within the infarcted foci of the left ventricle. There was no significant difference in the infarct ratios between Groups A and B (P=0.1741). The infarct ratios of Groups C and D were lower than those of Groups A (1.76±0.73% vs. 12.83±4.29%, P=0.0116; 1.88±0.40% vs. 12.83±4.29%, P=0.0116) and B (1.76±0.73% vs. 8.21±2.27%, P=0.0094; 1.88±0.40% vs. 8.21±2.27%, P=0.0089). There was no significant difference between Groups C and D (P=0.8244).

HE staining (100×) and immunohistochemical analysis of GFP are shown in **Figure 4**. The myocardium was replaced by fibrous scar tissue within the infarcted foci of the four groups. GFP-positive cardiomyocytes were found within the infarcted foci from Group B, indicating the differentiation of transplanted GFP/Fluc-BMSCs into cardiomyocytes. GFP-positive cells were also found in Groups C and D. No GFP-positive cells were found in Group A.

Immunohistochemical analysis of CD34 from Group A (100×) is shown in **Figure 5A** as an example, and the MVDs of the four groups in **Figure 5B**. The MVDs of Groups B, C and D were higher than that of Group A (7.27±0.47% vs. 5.40±0.40%, P=0.0064; 9.17±0.15% vs. 5.40±0.40%, P=0.0001; 9.73±0.40% vs. 5.40±0.40%, P=0.0002), and the MVDs of Groups C and D were higher than that of Group B (9.17±0.15% vs. 7.27±0.47%, P=0.0027; 9.73±0.40% vs. 7.27±0.47%, P=0.0024). There was no significant difference between Groups C and D (P=0.0856).

Discussion

Based on dual-modal imaging *in vivo* using BLI and MRI, we showed the feasibility of injectable functionalized self-assembling peptide nanofiber scaffold to improve the localization, survival and therapeutic effect of BMSCs to treat myocardial infarction.

Permanent loss of cardiomyocytes and scar tissue formation after MI results in an irreversible damage to the cardiac function. Cardiac repair (replacement, restoration, and regeneration) is, therefore, essential to restore function of the heart following MI. Current therapies are with lower early mortality rates. Thus, the myocardial tissue regeneration with the application of stem cells is an effective therapeutic option [16]. The ability to improve cardiac function with the stem cell-based therapy needs to be further addressed [16]. A long-term retention within the injection site is necessary for a consistent benefit to treat myocardial infarction [17, 18]. This study showed that the transplant-

ed BMSCs did localize and proliferate in the myocardium, but their levels soon decreased and fell below the detection threshold within the second week. Moreover, there is no not statistical significance in therapy response compared BMSCs Group B with that of Group A.

It has been proven that co-therapy with supplements, such as antioxidants [19], immune-suppressants [20], and growth factors [21] could lengthen the survival of stem cells and strengthen their therapeutic effects. Recently, the studies showed that the special scaffolds could provide a better living environment for transplanted stem cells [22, 23]. In this study, a type of functionalized self-assembling peptidenanofiber was used, which can function as a combination of scaffold and supplements. These nanofibers have the same frame, RADA16-I, which is soluble in water and will convert to hydrogels physically mimics the natural extracellular matrix under physiological conditions. Such a property makes in situ injection more convenient than other scaffolds in solid form. The frame can be easily functionalized by adding various bioactive peptide motifs [13]. RAD/PRG was chosen because it improved the survival of stem cells best in 3-D culture [12], and RAD/KLT has been demonstrated that it recruited endothelial cells and induced subsequent angiogenesis [11]. In this study, our results showed that when co-transplanted with RAD/PRG, the BLI signal of GFP/Fluc-BMSCs in Group C was significantly strengthened and lengthened, the LVEF value after transplantation was significantly improved, and the infarct ratio was significantly reduced, compared with those in Group A and Group B, respectively. When co-transplanted with RAD/KLT (Group D), the MVD was significantly higher, the LVEF value after transplantation was also significantly improved, and the infarct ratio was significantly reduced compared with those in Group A and Group B, respectively. This is the first study, in our acknowledgements, the functionalized self-assembling peptide nanofiber RAD/PRG or RAD/KLT is applied to treat AMI, the results encourage us to develop and investigate a series of functionalized self-assembling peptide nanofiber scaffolds in the future.

Another key factor is the functional mechanism of stem cells to treat AMI. The results of this study showed that BMSCs might function via differentiation and angiogenesis. Immunohistochemical analysis of GFP *ex vivo* showed GFP-positive cardiomyocytes within the infarcted foci, indicating the differentiation of transplanted GFP/Fluc-BMSCs into cardiomyocytes. However, BMSCs, similar to SMs, adipose-derived stem cells (ADSCs), and induced pluripotent stem cells (iPSCs), are not cardiac resident stem cells. BMSCs are distributed throughout the body before extraction and can be recruited again by other organs through blood flow after transplantation into the heart [6]. BLI signals were detected in the cardiac region in all the experimental groups, indicating the distribution of BMSCs throughout the whole body. The relatively low retention within the myocardium is not sufficient to explain the improvement in cardiac function [24]. However, studies have shown that BMSCs secrete a series of cytokines by paracrine action to protect the ischemic cardiomyocytes from apoptosis and inflammation, to induce angiogenesis for tissue repair, and to recruit resident cardiac stem cells into action [25, 26]. Once the reparative procedure is initiated, BMSCs themselves withdraw, explaining why signals of BMSCs disappear early.

In this study, immunohistochemical analysis of CD34 and quantification showed that the MVDs of Groups B, C and D were significant higher than that of Group A, and the MVDs of Groups C and D were significant higher than that of Group B. The angiogenesis of Group D occurred through a VEGF-like mechanism involving RAD/KLT, and the angiogenesis of Group B could only be attributed to GFP/Fluc-BMSCs; particularly, when the survival of GFP/Fluc-BMSCs was promoted by RAD/PRG in Group C, the MVD increased further.

This study possesses limitations. This is the first trial to co-transplant BMSCs with functionalized self-assembling peptide nanofibers RAD/PRG and RAD/KLT. A small sample and short-term follow-up were applied to validate our conception, its usefulness should be examined big samples with long-term follow-up in future studies. Second, rat GFP/Fluc-BMSCs were used in mouse AMI model. Xenotransplantation could induce immunological rejection. However, the immunogenicity of BMSCs is thought to be low because of incomplete expression of histocompatibility antigen [27, 28]. Successful transplantations of heterogeneous BMSCs have been reported in preclinical and clinical set-

tings [27, 28]. Additionally, during the establishment of the AMI model, the mouse thymus was resected before expose the heart, a process that can weaken the immunological reaction [29]. Third, we hypothesize that BMSCs function by differentiation and paracrine signaling using HE staining and immunohistochemical analysis. Further studies, additional ELISA and immunofluorescence will bring other stronger evidence.

In conclusion, based on dual-modal imaging using BLI and MRI, the localization and survival of BMSCs in the infarcted myocardium was promoted by co-transplantation with RAD/PRG, and the therapeutic effect was enhanced by co-transplantation with either RAD/PRG or RAD/KLT. Functionalized self-assembling peptide nanofibers have been proven to be of good biological histocompatibility, and significant ability to support the proliferation and differentiation of stem cells for nervous tissue repair in animal studies. Now they are in the threshold for cardiovascular disease. When stem cell therapy falls into a bottleneck, we see a bright future with new ideas from biomaterials and tissue engineering.

Acknowledgements

This work is supported by the National Natural Science Foundation of China (2015, Grant NO. 81471725), the Health Industry Special Scientific Research Project (201402019) and the Tsinghua University Initiative Scientific Research Program (20121087982, 20131089199). Dr. Di Dong from the Key Laboratory of Molecular Imaging, Institute of Automation, Chinese Academy of Sciences, Beijing, China assisted in the bioluminescence imaging.

Disclosure of conflict of interest

None.

Address correspondence to: Dr. Yi-Ning Wang, Department of Radiology, Peking Union Medical College Hospital, Chinese Academy of Medical Sciences and Peking Union Medical College, No. 1, Shuaifuyuan, Dongcheng District, Beijing 100730, China. Tel: +86-010-69155509; Fax: +86-010-69155441; E-mail: wangyining@pumch.cn; Dr. Xiu-Mei Wang, Key Laboratory of Advanced Materials, School of Materials Science and Engineering, Tsinghua University, Beijing 100084, China. Tel: +86-010-62782966; Fax: +86-010-62771160; E-mail: wxm@mail.tsinghua.edu.cn

References

[1] Jeevanantham V, Butler M, Saad A, Abdel-Latif A, Zuba-Surma EK and Dawn B. Adult bone marrow cell therapy improves survival and induces long-term improvement in cardiac parameters: a systematic review and meta-analysis. Circulation 2012; 126: 551-568.

[2] Makkar RR, Smith RR, Cheng K, Malliaras K, Thomson LE, Berman D, Czer LS, Marban L, Mendizabal A, Johnston PV, Russell SD, Schuleri KH, Lardo AC, Gerstenblith G and Marban E. Intracoronary cardiosphere-derived cells for heart regeneration after myocardial infarction (CADUCEUS): a prospective, randomised phase 1 trial. Lancet 2012; 379: 895-904.

[3] Menasche P, Alfieri O, Janssens S, McKenna W, Reichenspurner H, Trinquart L, Vilquin JT, Marolleau JP, Seymour B, Larghero J, Lake S, Chatellier G, Solomon S, Desnos M and Hagege AA. The Myoblast Autologous Grafting in Ischemic Cardiomyopathy (MAGIC) trial: first randomized placebo-controlled study of myoblast transplantation. Circulation 2008; 117: 1189-1200.

[4] Kim J, Shapiro L and Flynn A. The clinical application of mesenchymal stem cells and cardiac stem cells as a therapy for cardiovascular disease. Pharmacol Ther 2015; 151: 8-15.

[5] Dixit P and Katare R. Challenges in identifying the best source of stem cells for cardiac regeneration therapy. Stem Cell Res Ther 2015; 6: 26.

[6] Nguyen PK, Riegler J and Wu JC. Stem cell imaging: from bench to bedside. Cell Stem Cell 2014; 14: 431-444.

[7] Menasche P. Stem cells for the treatment of heart failure. Philos Trans R Soc Lond B Biol Sci 2015; 370: 20140373.

[8] Garbern JC and Lee RT. Cardiac stem cell therapy and the promise of heart regeneration. Cell Stem Cell 2013; 12: 689-698.

[9] Nguyen PK, Lan F, Wang Y and Wu JC. Imaging: guiding the clinical translation of cardiac stem cell therapy. Circ Res 2011; 109: 962-979.

[10] Davis ME, Motion JP, Narmoneva DA, Takahashi T, Hakuno D, Kamm RD, Zhang S and Lee RT. Injectable self-assembling peptide nanofibers create intramyocardial microenvironments for endothelial cells. Circulation 2005; 111: 442-450.

[11] Liu X, Wang X, Horii A, Wang X, Qiao L, Zhang S and Cui FZ. In vivo studies on angiogenic activity of two designer self-assembling peptide scaffold hydrogels in the chicken embryo chorioallantoic membrane. Nanoscale 2012; 4: 2720-2727.

[12] Liu X, Wang X, Wang X, Ren H, He J, Qiao L and Cui FZ. Functionalized self-assembling peptide

nanofiber hydrogels mimic stem cell niche to control human adipose stem cell behavior in vitro. Acta Biomater 2013; 9: 6798-6805.
[13] Padin-Iruegas ME, Misao Y, Davis ME, Segers VF, Esposito G, Tokunou T, Urbanek K, Hosoda T, Rota M, Anversa P, Leri A, Lee RT and Kajstura J. Cardiac progenitor cells and biotinylated insulin-like growth factor-1 nanofibers improve endogenous and exogenous myocardial regeneration after infarction. Circulation 2009; 120: 876-887.
[14] Cao J, Li X, Chang N, Wang Y, Lei J, Zhao D, Gao K and Jin Z. Dual-modular molecular imaging to trace transplanted bone mesenchymal stromal cells in an acute myocardial infarction model. Cytotherapy 2015; 17: 1365-1373.
[15] Boopathy AV and Davis ME. Self-assembling peptide-based delivery of therapeutics for myocardial infarction. Methods Mol Biol 2014; 1141: 159-164.
[16] Feric NT and Radisic M. Strategies and challenges to myocardial replacement therapy. Stem Cells Transl Med 2016; 5: 410-416.
[17] Passier R, van Laake LW and Mummery CL. Stem-cell-based therapy and lessons from the heart. Nature 2008; 453: 322-329.
[18] Hu S, Huang M, Nguyen PK, Gong Y, Li Z, Jia F, Lan F, Liu J, Nag D, Robbins RC and Wu JC. Novel microRNA prosurvival cocktail for improving engraftment and function of cardiac progenitor cell transplantation. Circulation 2011; 124: S27-34.
[19] Rodriguez-Porcel M, Gheysens O, Paulmurugan R, Chen IY, Peterson KM, Willmann JK, Wu JC, Zhu X, Lerman LO and Gambhir SS. Antioxidants improve early survival of cardiomyoblasts after transplantation to the myocardium. Mol Imaging Biol 2010; 12: 325-334.
[20] Rong Z, Wang M, Hu Z, Stradner M, Zhu S, Kong H, Yi H, Goldrath A, Yang YG, Xu Y and Fu X. An effective approach to prevent immune rejection of human ESC-derived allografts. Cell Stem Cell 2014; 14: 121-130.
[21] Pourrajab F, Babaei Zarch M, Baghi Yazdi M, Rahimi Zarchi A and Vakili Zarch A. Application of stem cell/growth factor system, as a multimodal therapy approach in regenerative medicine to improve cell therapy yields. Int J Cardiol 2014; 173: 12-19.
[22] Xu Y, Patnaik S, Guo X, Li Z, Lo W, Butler R, Claude A, Liu Z, Zhang G, Liao J, Anderson PM and Guan J. Cardiac differentiation of cardiosphere-derived cells in scaffolds mimicking morphology of the cardiac extracellular matrix. Acta Biomater 2014; 10: 3449-3462.
[23] Ban K, Park HJ, Kim S, Andukuri A, Cho KW, Hwang JW, Cha HJ, Kim SY, Kim WS, Jun HW and Yoon YS. Cell therapy with embryonic stem cell-derived cardiomyocytes encapsulated in injectable nanomatrix gel enhances cell engraftment and promotes cardiac repair. ACS Nano 2014; 8: 10815-10825.
[24] Bolli R, Chugh AR, D'Amario D, Loughran JH, Stoddard MF, Ikram S, Beache GM, Wagner SG, Leri A, Hosoda T, Sanada F, Elmore JB, Goichberg P, Cappetta D, Solankhi NK, Fahsah I, Rokosh DG, Slaughter MS, Kajstura J and Anversa P. Cardiac stem cells in patients with ischaemic cardiomyopathy (SCIPIO): initial results of a randomised phase 1 trial. Lancet 2011; 378: 1847-1857.
[25] Duran JM, Makarewich CA, Sharp TE, Starosta T, Zhu F, Hoffman NE, Chiba Y, Madesh M, Berretta RM, Kubo H and Houser SR. Bone-derived stem cells repair the heart after myocardial infarction through transdifferentiation and paracrine signaling mechanisms. Circ Res 2013; 113: 539-552.
[26] Williams AR, Hatzistergos KE, Addicott B, McCall F, Carvalho D, Suncion V, Morales AR, Da Silva J, Sussman MA, Heldman AW and Hare JM. Enhanced effect of combining human cardiac stem cells and bone marrow mesenchymal stem cells to reduce infarct size and to restore cardiac function after myocardial infarction. Circulation 2013; 127: 213-223.
[27] Liu J, Narsinh KH, Lan F, Wang L, Nguyen PK, Hu S, Lee A, Han L, Gong Y, Huang M, Nag D, Rosenberg J, Chouldechova A, Robbins RC and Wu JC. Early stem cell engraftment predicts late cardiac functional recovery: preclinical insights from molecular imaging. Circ Cardiovasc Imaging 2012; 5: 481-490.
[28] Hare JM, Fishman JE, Gerstenblith G, DiFede Velazquez DL, Zambrano JP, Suncion VY, Tracy M, Ghersin E, Johnston PV, Brinker JA, Breton E, Davis-Sproul J, Schulman IH, Byrnes J, Mendizabal AM, Lowery MH, Rouy D, Altman P, Wong Po Foo C, Ruiz P, Amador A, Da Silva J, McNiece IK, Heldman AW, George R and Lardo A. Comparison of allogeneic vs autologous bone marrow-derived mesenchymal stem cells delivered by transendocardial injection in patients with ischemic cardiomyopathy: the POSEIDON randomized trial. JAMA 2012; 308: 2369-2379.
[29] Gratz IK, Rosenblum MD and Abbas AK. The life of regulatory T cells. Ann N Y Acad Sci 2013; 1283: 8-12.